Supporting Online Material for

Atomic Description of an Enzyme Reaction Dominated by Proton Tunneling

Laura Masgrau,* Anna Roujeinikova, Linus O. Johannissen, Parvinder Hothi, Jaswir Basran, Kara E. Ranaghan, Adrian J. Mulholland,* Michael J. Sutcliffe,* Nigel S. Scrutton,* David Leys*

*To whom correspondence should be addressed. E-mail: david.leys@manchester.ac.uk (D.L.); michael.sutcliffe@manchester.ac.uk (M.J.S.); adrian.mulholland@bristol.ac.uk (A.J.M.); nigel.scrutton@manchester.ac.uk (N.S.S.)

Published 14 April 2006, *Science* **312**, 237 (2006)
DOI: 10.1126/science.1126002

This PDF file includes:

Supporting Online Material

for

“Atomic description of an enzyme reaction dominated by proton tunnelling”

Contents

Materials and Methods

Protein purification and preparation of crystals

AADH was purified from *Alcaligenes faecalis* IFO 14479 as described *(1).* For crystallization, the purified protein was oxidised with 1 mM potassium ferricyanide, exchanged into 10 mM potassium phosphate buffer pH 7.5 by gel exclusion chromatography and concentrated to 20 mg/ml (estimated using an extinction coefficient of 27,600 M^{-1} cm^{-1} at 433 nm). Dark-green-coloured crystals of oxidised AADH were produced by the sitting drop vapor diffusion technique using 19-25% (w/v) PEG 2000 monomethylether, 100 mM ammonium sulphate and 100 mM sodium cacodylate pH 6.0 as a reservoir solution. Crystals (form A) belong to space group $P2_1$ with unit cell parameters a=70.8, b=89.1, c=80.3 Å, β=90.2° and contain a heterotetramer in the asymmetric unit. Crystals of the phenylhydrazine adduct and tryptamine-reduced AADH were produced by soaking the form A crystals in a stabilising solution that included either 40 mM phenylhydrazine (15 min) or 100 mM tryptamine (3 days). Crystals of the Schiff base and carbinolamine intermediates of AADH were obtained either by soaking of the form A crystals in 100 mM tryptamine solution and flash-cooling immediately after TTQ reduction was observed (crystal turn colourless) or after a period of 5-10 min had passed subsequent to full reduction. Alternatively, crystal structures were obtained co-crystallization with tryptamine under strict anaerobic conditions. For co-crystallization, the reservoir solution was of a very similar content to that used for oxidised AADH. Protein solution (12.5 mg/ml) was incubated with tryptamine (5 mM) for 15 min and then dialysed anaerobically overnight against 10 mM potassium phosphate, pH 7.5, to remove excess substrate prior to crystallization. Form B crystals ($P2_12_12_1$, a=90.4, b=96.2, c=120.3 Å, one heterotetramer per asymmetric unit) were obtained using 19-21% (w/v) PEG 2K MME; form C crystals (F222, a=119.9, b=157.3, c=268.0 Å, one heterotetramer per asymmetric unit) were obtained using 25-27% PEG 2K MME. Crystals of form B and

C were flash-cooled in liquid nitrogen 12 days after setting up the crystallization trials.

Data collection and structure determination

Diffraction data were collected at cryogenic temperatures on ESRF stations ID14-1 and 14-2 (Grenoble, France) and DESY-EMBL station X11 (Hamburg, Germany). All data were processed and scaled using the DENZO/SCALEPACK package *(2)* (Table S3). The structure of AADH was determined by the MIR technique using form A crystals. The overall figure of merit of the experimental phase set to 2.3 Å was 0.37. An improved map was obtained by combined solvent flattening, histogram matching and 2-fold non-crystallographic symmetry averaging as implemented in DM *(3),* with a solvent content of 40 %. Model building and refinement were carried out using programs TURBO-FRODO *(4),* WARPNTRACE *(5)* and REFMAC *(6);* stereochemistry was analysed by PROCHECK *(7)* (Table S4). High resolution Fourier difference maps allowed unambiguous identification of the species present in the active site. In all models – with the exception of the lower resolution Schiff base form B intermediate – hydrogen atoms were included in the last stages of refinement in their riding positions as implemented in REFMAC. The structure of the free enzyme was used as the starting model for refinement of the phenylhydrazine complex and the intermediates produced by soaking. The form B and C crystal structures were solved by the molecular replacement technique (AmoRe *(8)*) using the form A structure as a search model. Electron density clearly identified a Schiff base intermediate in the form B crystals and a carbinolamine intermediate in the form C. To avoid X-ray induced radiation damage atomic resolution data were collected with periodic translation of the crystal to minimize X-ray dose received. No evidence for X-ray induced radiation damage at the active site was detected and no significant difference could be found as a function of X-ray dose, with the exception of the unavoidable rapid reduction by X-rays of the unsoaked oxidized crystals.

Computational simulations

The tryptamine-derived iminoquinone complex (III), the starting point of all our simulations, was built, following standard procedures with CHARMM, from the 1.1 Å structure of the Schiff base intermediate V. That the C1-O1 and C1-O2 (intermediate V) and the corresponding N-O1 and N-O2 (intermediate III phenylhydrazine analog) distances are essentially identical gives us confidence that the modelled tryptamine-derived iminoquinone complex (III) is an accurate representation of the 'true' structure of intermediate III. In the QM/MM calculations, the QM region (Fig. S2) contained 45 atoms and was linked to the rest of the system by three HQ-type link atoms *(9)*. The QM/MM (PM3/CHARMM22 using CHARMM *(10)*) classical free energy was calculated along the (approximate) reaction coordinate Z = [R(C-H) – R(O-H)] using a 25 Å radius sphere simulation system centred on N of the iminoquinone, with each Z-value window sampled for up to 30 ps of stochastic boundary molecular dynamics, using techniques similar to ref.*11*. The barrier height was corrected based on higher level quantum chemical results obtained for the similar methylamine dehydrogenase–methylamine system *(12)* to give the classical free energy of activation, $\Delta G^{\ddagger,classical}$. $\Delta G^{\ddagger,tunnelling}$ was estimated from VTST/SCT calculations *(13,14),* in which a minimum energy path was obtained for each reaction and each isotopic substitution with the QM atoms embedded in the potential of the fixed MM atoms, using the CHARMMRATE interface*(15)* and applying the corrections mentioned above, using the interpolated single point energies algorithm *(16)* in POLYRATE *(17)*. 7 ns of MM (CHARMM22) molecular dynamics were performed for the $\alpha_2\beta_2$ heterotetramer for the iminoquinone (III), including crystal waters; dynamical cross-correlation analysis *(18),* principal components analysis on the last 4 ns of each trajectory, and spectral densities *(19)* of the motions were calculated for a 400 ps window (2.0 to 2.4 ns) with coordinates recorded every 4 fs; digital filtering *(20)* was applied to the same 400 ps window. PM3/CHARMM22 molecular dynamics simulations were performed for the unrestrained product (IV) and for the complex V generated by proton rearrangement

in IV. The structures in these trajectories were used to calculate the average electrostatic stabilisation of Asp128β by Trp160β and Thr172β in these two complexes. All calculations were performed at 300 K.

References

1. S. Govindaraj, *J. Bacteriol.* **176**, 2922 (1994).
2. Z. Otwinowski, W. Minor, *Method. Enzymol.* **276**, 307 (1997).
3. Cowtan, K. *Joint CCP4 ESF EACBM Newsletter Protein Crystallog.* **31**, 34 (1994).
4. A. Roussel, C. Cambillau, C. in *Silicon Graphics Geometry Partners Directory 86.* (Silicon Graphics, Mountain View, CA, USA, 1991).
5. A. Perrakis, R. Morris, V.S. Lamzin, *Nat. Struct. Biol.* **6**, 458 (1999).
6. G.N. Murshudov, A.A. Vagin, E.J. Dodson, *Acta Crystallogr. D* **53**, 240 (1997).
7. R.A.Laskowski, M.W. Macarthur, D.S. Moss, J.M. Thornton, *J. Appl. Crystallogr.* **26**, 283 (1993).
8. J. Navaza, J. *Acta Crystallogr. A* **50**, 157 (1994).
9. M.J. Field, P.A. Bash, M.A. Karplus, *J. Comput. Chem.* **11**, 700 (1990).
10. B.R. Brooks, et al. *J. Comput. Chem.* **4**, 187 (1983).
11. L. Ridder, I.M.C.M. Rietjens, J. Vervoort, A.J. Mulholland, *J. Am. Chem. Soc.* **124**, 9926 (2002).
12. G. Tresadern, H. Wang, P.F. Faulder, N.A. Burton, I.H. Hillier, *Mol. Phys.* **101**, 2775 (2003).
13. D.G. Truhlar, B.C. Garrett, S.J. Klippenstein, *J. Phys. Chem.* **100**, 12771 (1996).
14. D.G. Truhlar, A.D. Isaacson, B.C. Garret, *Theory of Chemical Reaction Dynamics* (ed. Baer, M.) 65-136 (CRC Press, Boca Raton, FL, 1985).
15. C. Alhambra, et al. CHARMMRATE. University of Minnesota, Minneapolis. (2001)
16. Y.Y. Chuang, J.C. Corchado, D.G. Truhlar, *J. Phys. Chem. A* **103**, 1140 (1999).
17. J.C. Corchado, et al. POLYRATE. University of Minnesota, Minneapolis. (2000)
18. J.L. Radkiewicz, C.L. Brooks, *J. Am. Chem. Soc.* **122**, 225 (2000).
19. S. Caratzoulas, J.S. Mincer, S.D. Schwartz, *J. Am. Chem. Soc.* **124**, 3270 (2002).
20. R. B. Sessions, P. Dauberosguthorpe, D. J. Osguthorpe, *J. Mol. Biol.* **210**, 617 (1989).

Supplementary Data

MALDI-TOF MS of covalent reduced enzyme intermediate VII

To establish whether intermediate VII is stable in solution, we performed mass spectrometry of the enzyme reduced by substrate.

Material and methods:

MALDI-TOF MS was performed on a Bruker BiFLEX III mass spectrometer operating in linear mode. 1 μL of sample was applied to the MALDI target and allowed to dry. An equal volume of sinapinic acid (10 mg/mL in 60% acetonitrile/40% 0.1%TFA) was added and the solution dried in air. A composite spectrum was constructed resulting from the summation of 20-30 337 nm laser pulses. The AADH sample comprised 10 μM AADH contained in 20 mM ammonium bicarbonate, pH 7.8. Samples of substrate-reduced AADH were prepared by incubating the enzyme solution with a 4-fold excess of substrate for 15 minutes at room temperature.

Results and discussion:

The mass spectrometry data (Supplementary Data Table SD1) clearly indicate covalent modification of the enzyme as a consequence of incubating with aromatic amines (tryptamine and tyramine were analysed). The observed mass differences correspond with those expected for the respective intermediate VII and support the present model.

Supplementary Data Table SD1

Sample	**Observed molecular weight (Da)**	**Difference with reduced AADH (Da)**	**Expected difference for intermediate VII (Da)**
Reduced AADH	14478	-	-
AADH + tryptamine	14638	160	160
AADH + tyramine	14608	132	137

Figure S1

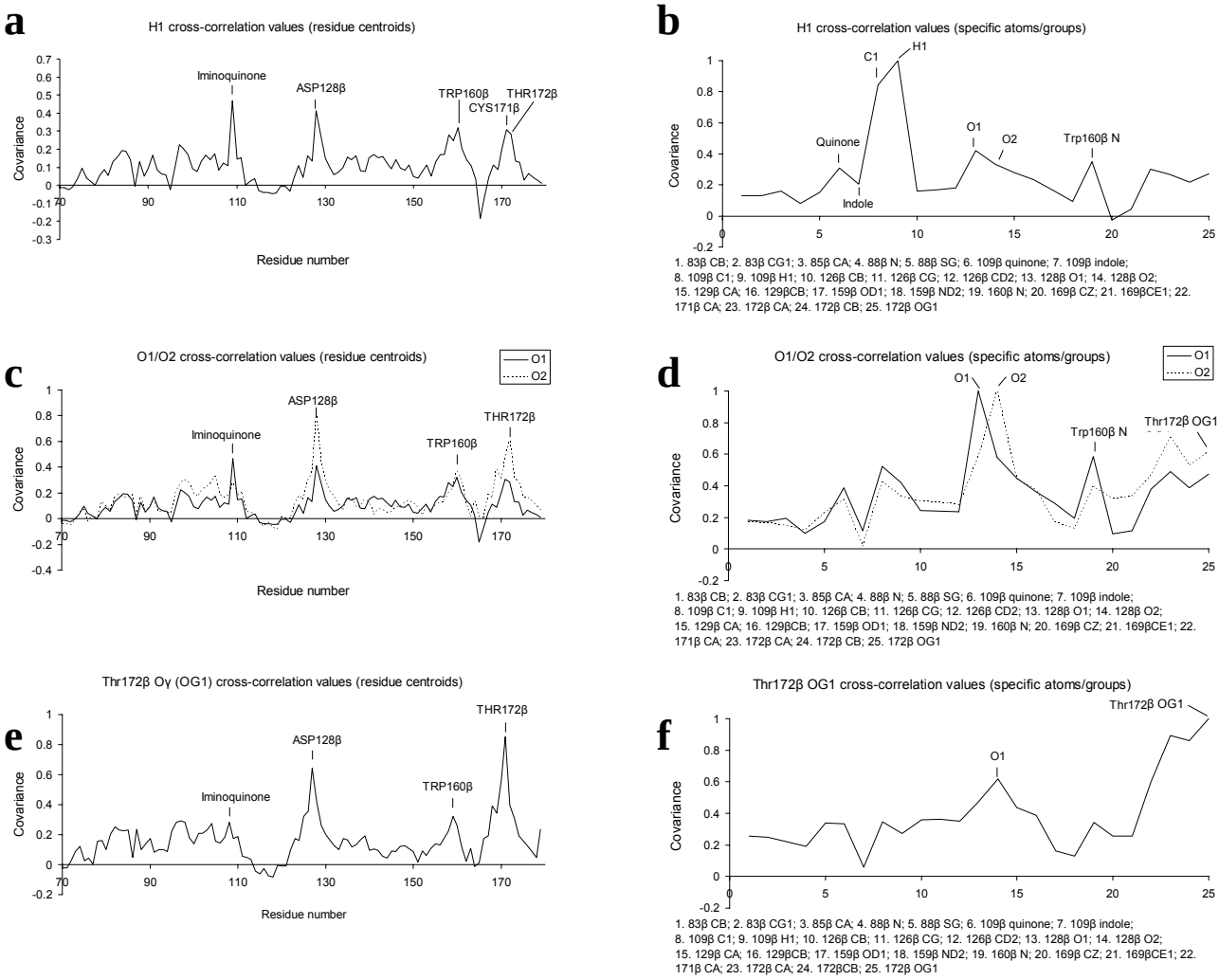

Cross-correlation coefficients from the MM MD simulation for iminoquinone C1/H1 (**a,b**), Asp128β O1/O2 (**c,d**) and Thr172β OG1, for motions of the residue centroids (**a**, **c, e**) and motions of specific atoms/groups of atoms around the active site (**b**, **d, f**). Cross-correlations are shown only for the β-subunit, since no residues from the α-subunit are in contact with C1/H1 or O1/O2, and the substrate indole, which is at the interface between the two subunits, is not significantly correlated with C1/H1 or O1/O2 and is not correlated with motions of the closest residues from the α-subunit (<0.2).

Note: A cross-correlation coefficient of 1 shows perfect correlation. Values close to 1 show a high degree of correlation, *e.g.*in (**b**) C1 is highly correlated to H1 (they are bonded). Even when a relatively low cut-off cross-correlation value of 0.5 is used, very little correlation is observed.

Figure S2

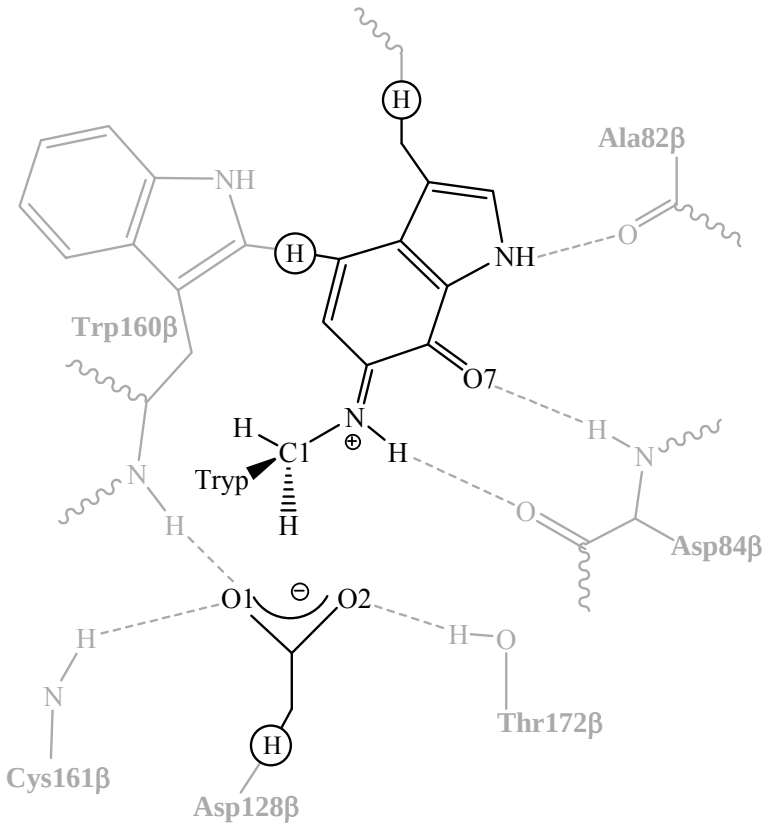

Schematic of the active site in iminoquinone III, illustrating the QM/MM partition used in the calculations. The QM region is shown in black and part of the surrounding MM region in grey with link atoms circled; hydrogen bonds between the QM region and active site residues are depicted by dashed lines.

Table S1: Kinetic data for the reaction of AADH with tryptamine

Protiated tryptamine

Temp (^{o}C)	Temp (K)	Temp (1000/K)	k_{obs} (s^{-1})[1,2,3]	ln (k/T)
3.0	276	3.62	527 ± 20 (8)[3]	0.6468
6.0	279	3.58	648 ± 39 (10)	0.8427
9.0	282	3.55	928 ± 93 (10)	1.1911
12.0	285	3.51	1294 ± 156 (9)	1.5130
15.0	288	3.47	1647 ± 121 (13)	1.7438
18.0	291	3.44	2010 ± 232 (11)	1.9326
21.0	294	3.40	2366 ± 338 (7)	2.0853

Deuterated tryptamine

Temp (^{o}C)	Temp (K)	Temp (1000/K)	k_{obs} (s^{-1})	ln (k/T)
5.0	278	3.60	9.483 ± 0.1 (5)	-3.38
10.0	283	3.53	14.92 ± 0.2 (5)	-2.94
15.0	288	3.47	21.06 ± 0.5 (5)	-2.62
20.0	293	3.41	30.02 ± 1.0 (5)	-2.28
25.0	298	3.36	47.84± 0.8 (5)	-1.83
30.0	303	3.30	71.02 ± 3.3 (5)	-1.45
35.0	308	3.25	101.2 ± 1.5 (5)	-1.11
40.0	313	3.19	141.2 ± 2.7 (5)	-0.8

[1]The rate of reduction of the TTQ centre, which is concerted with C-H/C-D bond cleavage, was measured using stopped-flow methods using an Applied Photophysics SX.18MV stopped-flow spectrophotometer. Reactions were conducted in 10 mM bis tris propane buffer, pH 7.5 and monitored as absorption bleaching at 456 nm. AADH concentration in the reaction chamber was 1.3 μM; substrate concentration was 180 μM. At least five replica

measurements were collected and averaged for each temperature. Analysis of reaction transients was as described (ref. 1). Enzymes were equilibrated for 10 minutes in the stopped-flow apparatus at the appropriate temperature prior to the acquisition of stopped-flow data. The optimal time for equilibration was determined empirically. Temperature control was achieved using a thermostatic circulating water bath and the temperature was monitored directly in the stopped-flow apparatus using a semiconductor sensor. In studies of the temperature dependence of bond cleavage, all substrates were used at saturating concentrations. Studies of the concentration dependence of bond cleavage at each temperature indicated that the apparent enzyme-substrate dissociation constant was not substantially perturbed on changing temperature. These control experiments ensured that substrate was saturating at all the temperatures investigated.

[2]The dead time of the stopped-flow instrument was 500 μs. Errors for protiated points at elevated temperatures are larger than those (i) at lower temperature and (ii) for deuterated substrate. This arises owing to the technical; difficulties associated with measuring rate constants > 1000 s^{-1} by the stopped-flow method.

[3]Quasithermodynamic parameters[5]: $\Delta H^{\ddagger\,(C\text{-}H)}$ = 57.3 ± 3.4 kJ/mol; $\Delta H^{\ddagger\,(D\text{-}H)}$ = 53.5 ± 1.2 kJ/mol; $\ln(A'^{H})$ = 25.6 ± 1.4; $\ln(A'^{D})$= 19.79 ± 0.49.

[4]Numbers in parentheses = number of traces averaged

[5]Temperature-dependent rate data can be plotted conveniently using the following form of the Eyring equation:

$$\ln(k/T) = \ln(k_B/h) + \Delta S^{\ddagger}/R - \Delta H^{\ddagger}/RT$$

The enthalpy of activation $\Delta H^{\ddagger}$ is calculated from the slope of the plot. As discussed previously (ref. 2), the use of this equation in plotting the temperature dependence of a unimolecular reaction is preferred over the use of the classical Arrhenius plot. This arises because the Arrhenius equation is in fact curved (although it appears linear in the accessible temperature range) and asymptotically approaches infinity at high temperatures. A consequence of using this form of the Eyring equation is the need to define explicitly the meaning of values obtained from such plots. Use of the Arrhenius plot has led to the development of criteria to indicate tunnelling based on the values for $\Delta\Delta E_a$ (~ 0 kJ/mol) and the A^H:A^D ratio (calculated from the intercepts of the Arrhenius plot for protium and deuterium substrates; >> 1 for a reaction proceeding purely by tunnelling, < 1 for moderate tunnelling). The corresponding parameters calculated from the slopes and intercepts of plots using the Eyring equation are $\Delta\Delta H^{\ddagger}$and A'^{H}:A'^{D} (the prime is used to distinguish this ratio from the A^H:A^D ratio calculated from the Arrhenius plot).

1. J. Basran, S. Patel, M. J. Sutcliffe, N. S. Scrutton, *J. Biol. Chem.* **276**, 6234 (2001).

2. J. Basran, M.J. Sutcliffe, N.S. Scrutton, *Biochemistry* **38**, 3218 (1999).

Table S2: Principal component analysis of the covariance

To further elucidate whether the motion of H1 is concerted with motions of other groups nearby, principal component analysis of the covariance matrix for C1, H1, quinone and indole centroids, ASP128β centroid and O1 and O2 was carried out. This revealed, unlike other groups, that the motion of H1 (and C1) corresponds almost entirely to the first principal component (see below). This suggests that the motion of H1 (and C1) is independent of the other groups.

Group	Overlap of covariance with the first principal component[1]
H1	0.98
C1	0.99
Quinone centroid	0.19
Indole centroid	-0.18
Asp128β centroid	0.37
Asp128β O1	0.43
Asp128β O2	0.22

[1]PCA produces a point in seven-dimensional space corresponding to each of the groups in covariance space; the normalised dot product (cosine) of the vector for each of these points relative to the first principal component (PC1) is a measure of how closely each vector corresponds to PC1.

Table S3: Crystallographic data collection statistics

Structure	Space group	Resolution range (Å)	Completeness (%)	Observed reflections	Unique reflections	R_{merge}[1] (%)	I/σ(I)
Semiquinone(2AH1)	$P2_1$	15-1.2 (1.25-1.20)	95 (91)	835610	288444	5.8 (45.1)	12.5 (2.2)
III Phenylhydrazine (2AGL)	$P2_1$	30–1.4 (1.45-1.40)	97 (97)	599666	187796	6.2 (32.1)	16.3 (4.1)
V Schiff base (2AGY)	$P2_1$	15-1.1 (1.14-1.10)	92 (82)	920397	357148	6.1 (51.0)	11.1 (1.5)
V Schiff base (2AGX)	$P2_12_12_1$	30-2.2 (2.28-2.20)	91 (75)	233265	49153	10.0 (33.2)	12.6 (2.8)
VII Carbinolamine (2AH0)	$P2_1$	30-1.45 (1.50-1.45)	98 (82)	600898	174584	6.5 (42.3)	16.1 (2.1)
VII Carbinolamine (2AGZ)	F222	30-1.6 (1.66-1.60)	94 (96)	532092	154579	5.9 (41.0)	14.9 (3.0)
I Tryptamine (2AGW)	$P2_1$	30-1.45 (1.50-1.45)	96(97)	541673	170610	6.9(41.9)	19.3 (2.7)

[1] $R_{merge} = \Sigma_{hkl} | I_i - I_m | / \Sigma_{hkl} I_m$, where I_m is the mean intensity of the reflection. Numbers in parentheses indicate values for the highest resolution shell.

Table S4: Crystallographic refinement statistics

Structure	Resolution (Å)	R_{cryst}[1]	R_{free}[2]	Bond length rms deviation (Å)	Bond angle rms deviation (°)	No. of reflections used	Number of protein atoms	Number of water molecules	Average B (protein atoms) ($Å^2$)	Average B (water molecules) ($Å^2$)	B averaged over both ligands ($Å^2$)
Semiquinone (2AH1)	15–1.2	14.1	16.9	0.012	1.5	288444	7265	1744	16.2	32.1	-
III Phenylhydrazine (2AGL)	15–1.4	17.1	19.6	0.012	1.5	177982	7374	1073	16.1	26.6	20.7
V Schiff base (2AGY)	15-1.1	14.5	16.3	0.012	1.5	357148	7251	1512	21.5	37.4	28.0
V Schiff base (2AGX)	15-2.2	15.9	22.5	0.012	1.3	46524	7327	577	22.3	24.1	33.1
VII Carbinolamine (2AH0)	15-1.45	16.7	20.0	0.012	1.4	165394	7280	1347	18.1	32.0	32.4
VII Carbinolamine (2AGZ)	15-1.6	14.2	16.9	0.013	1.5	146580	7348	1284	18.7	35.1	24.1
I Tryptamine (2AGW)	15-1.45	16.4	19.4	0.013	1.5	161400	7368	1208	16.6	29.8	25.9

[1] $R_{cryst} = \Sigma||F_o|-F_c||/\Sigma|F_o|$; [2] R_{free} was calculated on 5% of the data omitted at random